Recent Progress in Microscale Modeling of RF Sheaths

J. R. Myra,[1,] D. Curreli,[2] M.T. Elias[2] and T. G. Jenkins [3]

[1]*Lodestar Research Corporation, Boulder, Colorado, 80301 USA*
[2]*University of Illinois at Urbana-Champaign, Urbana, IL 61821 USA*
[3]*Tech-X Corporation, Boulder, Colorado, 80303 USA*

May 2019

submitted to

AIP Conference Proceedings

DOE-ER/54392-95; ORNL/4000158507-4 LRC-19-181

LODESTAR RESEARCH CORPORATION
2400 Central Avenue
Boulder, Colorado 80301

Presented at the 23rd Topical Conference on Radiofrequency Power in Plasmas
Hefei, China, May 14-17, 2019, paper P2.13

Recent Progress in Microscale Modeling of RF Sheaths

J. R. Myra,[1, a)] D. Curreli,[2, b)] M.T. Elias[2, c)] and T. G. Jenkins [3, d)]

[1]*Lodestar Research Corporation, 2400 Central Ave. Suite P-5, Boulder, Colorado, 80301 USA*
[2]*University of Illinois at Urbana-Champaign, 104 S. Wright St, Urbana, IL 61821 USA*
[3]*Tech-X Corporation, 5621 Arapahoe Avenue Suite A, Boulder, Colorado, 80303 USA*

[a)]jrmyra@lodestar.com
[b)]dcurreli@illinois.edu
[c)]mtelias2@illinois.edu
[d)]tgjenkins@txcorp.com

Abstract. The microscale properties of RF sheaths in the ion cyclotron range of frequencies (ICRF) are investigated by means of analytical theory, nonlinear fluid and particle-in-cell (PIC) code modeling. Previous work that parametrized RF sheath properties, specifically the RF sheath impedance and the rectified (DC) sheath potential, is generalized to include the effect of net DC current flow through the sheath. Analytical results are presented in the low frequency limit where the displacement current is negligible, and tested against results from a fluid numerical model. It is shown that when the sheath draws DC electron current, the voltage rectification is reduced from the zero current case, and the electron admittance is increased. In separate but related work on the microscale model, selected cases have been simulated with PIC codes to validate, further illuminate and extend fluid model results and their parametrizations. Quantitative agreement in trends for voltage rectification and sheath admittance vs. RF driving voltage is found.

INTRODUCTION

Radio frequency (RF) waves in the ion cyclotron range of frequencies (ICRF) can provide robust and cost effective heating for present day and future devices. In some situations, however, ICRF power is associated with enhanced impurity sputtering, parasitic power dissipation, and "hot spots" on antenna launchers and other nearby material surfaces. [1] It is commonly thought that RF sheaths are responsible for many of these unwanted interactions. RF sheaths modify the plasma potential, typically enhancing the energy of ions impacting the surface, and increasing sputtering and erosion.

Sheaths exist on a short spatial scale, nominally the Debye scale, which is generally small compared with RF wavelengths and device-size scale lengths. This makes it possible to describe the effect of an RF sheath on the macroscopic RF wave propagation problem [2] in terms of a sheath boundary condition (BC), which can be cast into the form of an effective RF surface impedance.

In previous work, various forms of an RF sheath BC were proposed. Early work was relevant to the capacitive sheath limit, $\omega_{pi} < \omega$ where ω_{pi} is the ion plasma frequency and ω is the RF wave frequency.[3,4] More recently, [5,6] the sheath BC was generalized using a microscale time-dependent one-dimensional nonlinear fluid model. In that model, the RF sheath is completely characterized by four dimensionless parameters: (i) the ion mobility ω/ω_{pi0}, (ii) the ion magnetization Ω_i/ω_{pi0}, where Ω_i is the ion cyclotron frequency (iii) the magnetic field direction relative to the surface, $\mathbf{b}\cdot\mathbf{s}$ where $\mathbf{b} = \mathbf{B}/B$, and $\mathbf{s}$ is the unit normal vector of the surface pointing into the plasma, and (iv) the RF amplitude $\xi = eV_{rf}/T_e$ where V_{rf} is the zero-to-peak amplitude at the sheath entrance, and T_e is the electron temperature. Here ω_{pi0} is with respect to the upstream (quasi-neutral) plasma density n_{i0}. In the first part of the present paper, the previously developed sheath rectification and impedance model is extended to include a fifth parameter: the dimensionless DC current flowing through the sheath, $J_{DC}/n_{i0}ec_s$. This extension is motivated by the fact that RF-induced DC sheath currents have been inferred in experiments on AUG,[7] NSTX [8] and EAST [9].

The second part of this paper begins the process of verification and extension of the fluid model by employing particle-in-cell (PIC) simulations. The rectification and sheath admittance (reciprocal impedance) obtained from PIC simulations are compared with those obtained from the nonlinear fluid model.

FLUID SHEATH MODEL WITH NET DC CURRENT

We consider a double-plate model of the type employed in Refs. [5] and [6], namely, a plasma-filled "capacitor" immersed in an oblique angle magnetic field, driven by anti-symmetric RF voltages on each of the two plates. Particle and DC current sources are located at the midplane of the capacitor cell. The distance between the plates is large compared with both the Debye length and the ion Larmor radius, so that the sources exist in the upstream region outside the non-neutral sheath and magnetic presheath. The model is 1D with all quantities varying only in x, the direction normal to the plates.

The applied voltages on plates 1 and 2 are $V_1 = V_{rf} \sin \omega t$ and $V_2 = -V_{rf} \sin \omega t$ respectively. Thus the plates are at a DC potential of zero. In the absence of a DC current source, RF sheath rectification causes the DC upstream plasma potential Φ_0 to rise to a value of order V_{rf} when $eV_{rf} >> 3T_e$. The dependence of Φ_0 on the dimensionless parameters of the problem, including now, the DC current flowing through the sheath, is one of the desired outputs of the calculation. The other quantity of interest is the sheath admittance parameter z defined as the ratio of the RF current flowing through the sheath to the RF voltage across the sheath at frequency ω.

Dimensionless variables will be employed throughout this paper unless otherwise indicated. The normalization scales for time, space, density and voltage are respectively: the inverse ion plasma frequency $1/\omega_{pi0}$, the electron Debye length λ_{de0}, n_{i0} and T_e/e. The fundamental equations of the nonlinear fluid sheath model are Poisson's equation for the electrostatic potential Φ, the Maxwell-Boltzmann relation for electron density n_e, the continuity equation for ion density n_i, and the vector ion equation of motion under the Lorentz force.

The remaining equation, needed to determine the upstream potential Φ_0 is the ambipolarity condition $\nabla \cdot \mathbf{J} = 0$ where the current **J** includes electrons, ion and displacement current. Integrating over the volume and including the source contribution at the midplane one obtains

$$J_{x1} + J_{x2} = -2J_{DC} b_x \tag{1}$$

where J_{DC} is the dimensionless injected current, normalized to the ion saturation current, and $b_x = \mathbf{B}\cdot\mathbf{e}_x/B$. It can be shown that J_{DC} lies in the range $1-\mu \le J_{DC} \le 1$ where $\mu = (m_i/2\pi m_e)^{1/2}$. Here the x component of the current at plate 1 is given by [5]

$$J_{x1} = \mu b_x \exp(V_1 - \Phi_0) + n_{i1}u_{x1} - \partial_x \partial_t \Phi_1 \tag{2}$$

and subscript 1 indicates evaluation at the location of plate 1. In addition to Φ_0 the other output quantity of interest is the admittance parameter y defined by

$$y = \frac{2\langle J_{x1}\cos\varphi\rangle}{V_{rf}} + \frac{2i\langle J_{x1}\sin\varphi\rangle}{V_{rf}} \tag{3}$$

where $\varphi = \omega t$ is the RF phase and <…> indicates an average over φ on $[0,2\pi]$. Thus the model generalizes the one in Refs. [5,6] by J_{DC} but is otherwise identical.

In the low frequency limit $\omega << 1$, we can drop the displacement current in J_{x1}, and using the symmetry of the problem, $J_{x2}(\omega t) = -J_{x1}(\omega t+\pi)$, and also $n_{i1}u_{x1} = n_{i0}u_{x0} = u_{x0} = b_x u_{||0}$, where $n_{i0} = 1$ in dimensionless variables. After some algebra one obtains

$$\Phi_0 = \ln\left[\frac{\mu\cosh(V_{rf}\cos\varphi)}{1-J_{DC}}\right] \tag{4}$$

The electron admittance is obtained from Eq. (3) with $J_{x1} \rightarrow J_{ex1}$, i.e. the first term in Eq. (2). In this limit Im $y_e = 0$ and the real part is given by

$$y_e = \frac{2\mu b_x}{V_{rf}}\left\langle e^{V_{rf}\cos\varphi - \Phi_0}\cos\varphi\right\rangle \tag{5}$$

The integral may be computed numerically. These J_{DC} modifications to Φ_0 and y_e are straightforward to incorporate into the parametrizations given in Ref. [6]; J_{DC} also modifies y_i and y_d indirectly through their dependence on Φ_0 using functional forms given explicitly in Ref. [6].

Results from the analytical scaling, the parametrization, and from the nonlinear fluid code (NoFlu) (retaining displacement current) are shown in Fig. 1. Although there are small differences, the theory and its parametrization capture the trends quite well. When the sheath draws electron current ($J_{DC} < 0$), a smaller sheath potential drop is required to confine electrons (since more are allowed to escape). This results in reduced ion sputtering but may increase the heat flux carried by the electrons to the surface. Not surprisingly when more DC electron current is drawn, the sheath RF current also increases as reflected by the increase in absolute value of the admittance.

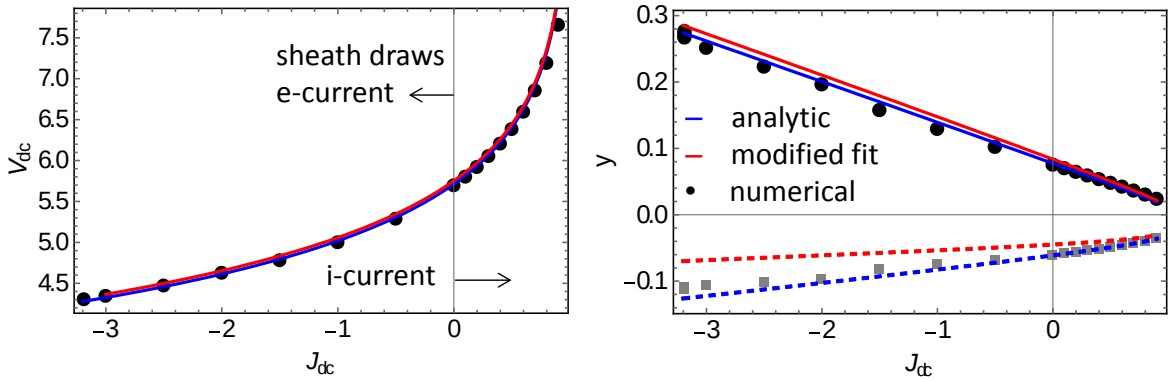

FIGURE 1. Rectified potential $V_{dc} = <\Phi_0>$ (left) and sheath admittance parameter y (right) vs. normalized sheath current J_{DC} for the parameters $\omega = 0.3$, $\Omega = 0.1$, $b_x = 0.2$ and $V_{rf} = 5$. Numerical results from the NoFlu code are shown as solid black disks, (and gray squares) the analytic scaling normalized to agree at $J_{DC} = 0$ is shown in blue and the parametrization is shown in red.

PIC SIMULATION RESULTS

PIC simulations of an RF sheath in double plate geometry have been carried out with the hPIC [10,11] and Vorpal [12] simulation codes. The goals of this part of the work are to verify fluid model results against microscale kinetic results, and to assess the importance of physics not in the fluid model, such as finite ion temperature, spatially distributed particle sources and fully kinetic (as opposed to Maxwell-Boltzmann) electrons.

The hPIC code is a fully-kinetic electrostatic Particle-in-Cell application targeted at large-scale simulations of Plasma–Material Interactions [10,11]. The code can simulate multi-component strongly-magnetized plasmas in a region close to the wall, including the magnetic sheath and presheath. The code has been adapted to include oscillating boundary conditions to analyze RF sheath problems. For the conditions relevant to this work, hPIC-RF operates with fully-kinetic ions and nonlinear Boltzmann electrons in the Poisson problem. A volumetric ionization source is used to replenish the particles lost to the walls. The ionization rate is tuned to maintain charge conservation in the plasma domain and thus maintain a constant average particle density in the plasma domain. hPIC-RF provides the energy angle distributions of the ions leaving the domain and impacting the walls, offering the opportunity to couple the code to codes for Plasma-Material Interactions [13,14]. Here we consider a 1D3V symmetric plate-to-plate collisionless hydrogen plasma configuration in a finite-size domain x=[0,L]=[0,3] cm with magnetic field B=1T parallel to the surface normal and plasma density of 5×10^{16} m^{-3}. The numerical discretization was set at 500 particles-per-cell and 20 time steps per ion gyroperiod. The plates oscillate at $V = \pm (V_{pp}/2) \sin \omega t$ volts where V_{pp} is the peak-to-peak RF voltage. The RF frequency is $\omega = 1.47\times10^{8}$ s^{-1} yielding $\omega/\omega_{pi0} = 0.5$.

Vorpal [12] is a massively parallel kinetic electromagnetics code based on finite-difference (FDTD) and particle-in-cell (PIC) methods. The Vorpal simulations performed for this paper used a PIC representation for both ions and electrons in the electrostatic approximation, contained between two infinite plates separated by 200 Debye lengths. Other parameters are the same as above and the case $V_{pp} = 200$ V is simulated. Numerically, the simulation grid resolves the Debye length (six grid cells per Debye length) and electron gyromotion (20 timesteps per gyro-orbit); with 10-500 particles per grid cell. In initial simulation efforts, particles lost to the wall were re-loaded into the domain on the following timestep to maintain the average species densities. However, this method exhibited considerable numerical noise and/or instability. To circumvent these issues, we instead added particles of both species into the domain at a fixed rate. The simulations were run until steady-state was achieved; the desired

average steady-state density of 5×10^{16} m^{-3} can be obtained by adjustment of the loading rate. Because the Vorpal simulations represent the electron distribution function kinetically, they are constrained to small time-steps so that the electron motion can be resolved. Computational requirements for these runs are thus greater than for the corresponding hPIC runs. We are currently investigating whether this kinetic representation of the electrons contributes any additional physical effects of interest to the sheath evolution.

Comparisons of the nonlinear fluid model (NoFlu) with the hPIC and Vorpal results for the normalized rectified sheath potential V_{DC}, i.e. the time-averaged (DC) upstream (midplane) potential, and the normalized sheath admittance y are shown in Fig. 2. Good quantitative agreement in trends for both quantities is indicated. There is a small offset that is being investigated, along with the lower rectification effect seen in the Vorpal simulations. Note that the hPIC results are insensitive to T_i at least for the $T_i < V_{pp}$ cases investigated.

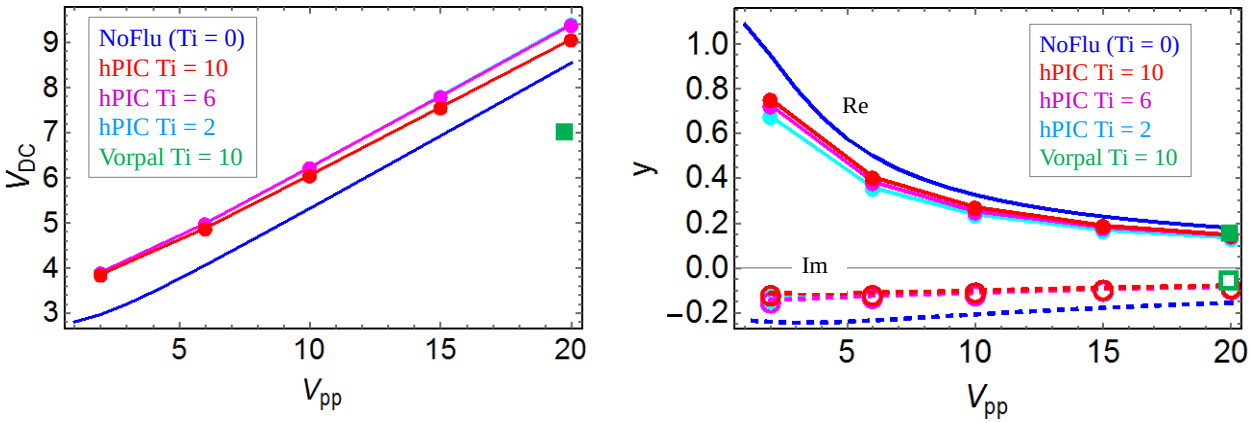

FIGURE 2. Normalized rectified potential $V_{DC} = <\Phi_0>$ (left) and normalized sheath admittance parameter y (right) vs. peak-to-peak RF voltage on the plates for the nonlinear fluid code (NoFLu) and the PIC codes hPIC and Vorpal.

ACKNOWLEDGMENTS

This material is based upon work supported by the U.S. Department of Energy Office of Science, Office of Fusion Energy Sciences under Award Numbers DE-FG02-97ER54392, DE-AC05-00OR2272/sub- 4000158507, DE-SC0018319 and DE-SC0018090-PO97564.

REFERENCES

1. J.-M. Noterdaeme and G. Van Oost, *Plasma Phys. Controlled Fusion* **35**, 1481 (1993).
2. H. Kohno and J. R. Myra, *Phys. Plasmas* **26**, 022507 (2019).
3. D. A. D'Ippolito and J. R. Myra, *Phys. Plasmas* **13**, 102508 (2006).
4. L. Colas, J. Jacquot, S. Heuraux, E. Faudot, et al., *Phys. Plasmas* **19**, 092505 (2012).
5. J. R. Myra and D. A. D'Ippolito, *Phys. Plasmas* **22**, 062507 (2015).
6. J. R. Myra, *Phys. Plasmas* **24**, 072507 (2017).
7. V. Bobkov, R. Bilato, L. Colas, R. Dux et al., *EPJ Web of Conferences* **157**, 03005 (2017).
8. R. J. Perkins, J.C. Hosea, M.A. Jaworski, R.E. Bell et al., *Nuclear Materials and Energy* **12**, 283 (2017).
9. R. J. Perkins, J. C. Hosea, G. Taylor, N. Bertelli et al., *Plasma Phys. Cont. Fusion* **61**, 045011 (2019).
10. R. Khaziev and D. Curreli, *Phys. Plasmas* **22**, 043503 (2015).
11. R. Khaziev and D. Curreli, *Comp. Phys. Commun.* **229**, 87 (2018).
12. C. Nieter and J. R. Cary, *J. Comp. Phys.* **196**, 448 (2004).
13. J. Drobny, A. Hayes and D. Curreli, D. N. Ruzic, *J. Nucl. Mater.* **494**, 278 (2017).
14. J. Drobny and D. Curreli , *Comp. Mater. Science* **149**, 301 (2018).